Design and Testing of an Adjustable Linkage for a Variable Displacement Pump

Shawn R. Wilhelm
e-mail: Wilh0141@UMN.EDU

James D. Van de Ven
Assistant Professor
e-mail: vandeven@UMN.EDU

Department of Mechanical Engineering,
University of Minnesota,
Minneapolis, MN 55455

A variable displacement hydraulic pump/motor with high efficiency at all operating conditions, including low displacement, is beneficial to multiple applications. Two major energy loss terms in conventional pumps are the friction and lubrication leakage in the kinematic joints. This paper presents the synthesis, analysis, and experimental validation of a variable displacement sixbar crank-rocker-slider mechanism that uses low friction pin joints instead of planar joints as seen in conventional variable pump/motor architectures. The novel linkage reaches true zero displacement with a constant top dead center position, further minimizing compressibility energy losses. The synthesis technique develops the range of motion for the base fourbar crank-rocker and creates a method of synthesizing the output slider dyad. It is shown that the mechanism can be optimized for minimum footprint and maximum stroke with a minimum base fourbar transmission angle of 30 deg and a resultant slider transmission angle of 52 deg. The synthesized linkage has a dimensionless stroke of 2.1 crank lengths with a variable timing ratio and velocity and acceleration profiles in the same order of magnitude as a comparable crank-slider mechanism. The kinematic and kinetic results from an experimental prototype linkage agree well with the model predictions. [DOI: 10.1115/1.4025122]

1 Introduction

Utilizing variable displacement hydraulic pumps and motors to control a hydraulic circuit offers significant energy savings over throttling valve control [1]. However, the efficiency of variable displacement machines decreases significantly at low displacement. This results in poor efficiency for applications that require operating at partial load for the majority of the cycle such as hydraulic hybrid vehicles, hydrostatic transmissions for wind power, and the unique application of compressed air energy storage using a liquid piston [2]. Thus, there is a general need to develop hydraulic pump/motors with high efficiency across the full displacement range.

There are three main architectures currently available for variable displacement pumps. An axial piston pump uses a variable angle swash plate to convert rotary motion into piston reciprocation resulting in fluid displacement. A bent axis piston pump uses a cylinder block, which is off-axis from the drive shaft. The bases of the pistons are mounted to a disk that is inline with the drive shaft while the piston heads are inline with the cylinder. All components rotate causing the pistons to reciprocate due to the bent axis. The angle between the input shaft and the cylinder determines the displacement. A vane pump has fluid chambers that are separated by vanes that are housed in a slotted rotor. The vanes contact a circular ring and the eccentricity between the ring and the rotor determines the fluid displacement [3]. All of these architectures utilize planar joints that suffer from a trade-off between high mechanical friction and high leakage to maintain hydrodynamic bearings. Much work has been done on improving the efficiency of these variable machines [4–9]. For the most part, these efforts have resulted in an increase in the maximum efficiency, but they have not addressed poor efficiency at low volumetric displacement. It is, therefore, reasonable to consider other methods of varying displacement.

An alternative approach to existing variable pump/motor architectures is to create an adjustable crank-slider linkage, which can vary its stroke and thus the displacement. Tao and Krishnamoorthy developed graphical synthesis technique for generating adjustable mechanisms with variable coupler curves [10,11]. McGovern and Sandor presented a method using complex numbers to analytically synthesize adjustable mechanisms for variable function and path generation [12,13]. Handra-Luca outlined a design procedure for sixbar mechanisms with adjustable oscillation angles [14]. Zhou and Ting presented a method of generating adjustable slider-crank mechanisms for multiple paths by adjusting the distance between the slider axis and the crank [15]. Recently, a number of adjustable four- and sixbar mechanisms have been presented, which vary the length of a moving link to change a coupler curve [16–22].

Adjustable linkage mechanisms for controlling piston displacement have been previously described and patented for internal combustions engines to vary the compression ratio to meet the power demand [23–28]. These engine linkages, however, do not go to zero displacement. Shoup developed a technique for the design of an adjustable spatial slider-crank mechanism for use in pumps or compressors [29]. This spatial mechanism requires the repositioning of the axis of slide relative to the crank. None of these mentioned techniques and examples provides both a constant top dead center (TDC) regardless of displacement and the ability to reach zero displacement. A preliminary kinematic synthesis technique was previously described by the authors [30], while this paper further expands the previous work with detailed analysis and experimental validation.

This paper describes the design of an adjustable sixbar slider linkage, which can drive a piston with a constant TDC and achieve zero displacement. In Sec. 2.1, a set of design requirements are presented, which drive the type synthesis. Section 2.2 describes the dimensional synthesis of the linkage. Sections 2.3 and 2.4 contain a kinematic analysis of the linkage. Section 2.5 presents and optimization of the linkage. Section 2.6 describes the dynamic analysis of an optimized linkage. Section 3 describes prototype design and experimental validation of the linkage model. Section 4 provides discussion and Sec. 5 contains concluding remarks.

Contributed by the Mechanisms and Robotics Committee of ASME for publication in the JOURNAL OF MECHANISMS AND ROBOTICS. Manuscript received August 2, 2012; final manuscript received July 15, 2013; published online September 11, 2013. Assoc. Editor: Jian S Dai.

2 Methods

2.1 Type Synthesis and Task Specifications. The concept of the linkage is to vary one of the links such that there is a change in the displacement or stroke of a slider (the piston). Several requirements must be defined to guide the synthesis process. For simplicity, variability will be achieved by moving a ground pivot rather than changing the length of a moving link. The axis of slide of the piston and the ground pivot of the crank will remain fixed to simplify the pump/motor block. Therefore, a third movable ground pivot is required for a functioning variable linkage. A minimal number of links is favorable as it limits the linkage's complexity, moving mass, and overall size. The three-ground pivot requirement limits the linkage options to either a Watt II or Stephenson III sixbar with a slider output. Of these two linkages, the Stephenson III seems more favorable because the ground pivot available for repositioning is attached to a binary link rather than a ternary link resulting in less moving mass to vary when the linkage is in motion.

With a linkage type selected, the next focus is on the task specifications. The first specification is that the output slider of the linkage must be able to reach a zero-displacement condition while the input crank continues to rotate. This is important because it allows the pump to go to a zero flow state. To create a slider mechanism with zero displacement, it is necessary for the coupler point to move in an arc about the pivot of the slider. As a result, the coupler point will not impart any translation on the slider. If a fourbar crank-rocker mechanism is constructed such that the coupler curve of any point on the coupler link is a pseudo-arc, and the slider pivot is placed at the center of this arc, then the slider of the resultant sixbar linkage would have approximately zero displacement. If the ground pivot of the rocker link of the base fourbar is moved, the coupler curve deviates from an arc and causes the slider to move.

The moving pivot, c, at the end of the rocker travels in a perfect arc about the ground pivot d as seen in Fig. 1. Thus, if the pin of the slider is located at point d, and this pin is connected to point c with an additional link, then the slider of the resultant mechanism exhibits zero displacement. In this configuration, the rocker link will be overlapping the connecting rod to the slider. This configuration is a hybrid between the Watt II and the Stephenson III.

The second task specification of focus is ensuring the piston returns the same position at the end of its stroke regardless of displacement. This position is defined as TDC. This is important because it minimizes the unswept volume of the pump chamber at any displacement, which reduces fluid compressibility losses. A more general case can be used to describe how this is accomplished. In any fourbar crank rocker, such as that in Fig. 1, for any position of the input link, θ_2, the precision position c will be at a defined position with resultant angles θ_3 and θ_4. If the ground pivot of link 4 is rotated about this point c such that there is an arc of d positions, then the coupler point will always return to this same position at the associated angle θ_2. While any θ_2 can be chosen, it is necessary to choose and angle such that the arc of d positions is created at the extreme positions of the coupler curve of point c. The process of determining θ_2 is discussed in more detail in Sec. 2.2.2. Another way of describing the location of the variable ground pivot d is through the ground link vector, $\vec{r}_1$, which connects the ground pivots a and d.

2.2 Dimensional Synthesis. With the type synthesis complete, and the method of achieving our task specifications known, dimensional synthesis is now presented to construct a feasible linkage solution. To represent this linkage mathematically, the input link is set to unity and all other lengths are a multiple of this value. The input crank ground position is defined to be the origin of a global coordinate system. The linkage is constructed in five steps: (1) The input fourbar crank-rocker is synthesized; (2) The timing of TDC is defined; (3) The variable ground pivot locations are found; (4) The location of zero displacement and axis of slide are defined; and (5) A resultant rocker-slider dyad is constructed.

The synthesis procedure is now explained in detail, using complex vector notation with appropriate rotation and stretch operators.

2.2.1 Variable Fourbar Synthesis. The base fourbar must be a crank-rocker and therefore meet the Grashof condition, which is defined by [31]

$$S + L \leq P + Q \tag{1}$$

where S is the length of the smallest link, L is the length of the longest link, and P and Q are the lengths of the remaining links. Another requirement of a crank-rocker is that link 2 is the shortest link [31]. With link 2 of unity length, the length of links 3 and 4 are free choices. The Grashof requirement defines the minimum and maximum possible lengths of the ground link where

$$r_{1\max} = P + Q - R_2 \tag{2}$$

$$r_{1\min} = r_2 + L - P \tag{3}$$

Doing so guarantees that the transmission angle will reach zero at $r_{1\max}$ and $r_{1\min}$, which can cause binding of the linkage. To avoid this, a minimum transmission angle, $\theta_{\min}$, is defined. From this transmission angle requirement, new values for $r_{1\min}$ and $r_{1\max}$ are created with a narrower range. These values are solved for by using the law of cosines with the geometry shown in Fig. 2.

Thus, the fourbar is defined with the range of acceptable values for the length of link 1 being $r_{1\min}$ to $r_{1\max}$. The point c will always travel in a circular arc with radius $|\vec{r}_4|$ about ground pivot d.

2.2.2 Defining Top Dead Center. To create an arc of positions of the ground pivot d that can be associated with TDC, the precision position c must be located at either end of the coupler curve. This occurs when $\vec{r}_2$ and $\vec{r}_3$ are collinear in either the extended case or the overlapping case as seen in Fig. 3. Selecting the extended or overlapped case is one of the free choices of the linkage synthesis. The collinear condition is required because the ends of the coupler curve represent the extreme positions of the rocker, which ultimately control the slider position of TDC and bottom dead center (BDC).

2.2.3 Find the Variable Ground Pivot Locations. With $r_{1\min}$, $r_{1\max}$, and the location of TDC defined, the arc of acceptable ground pivots can be defined. The adjustable ground pivot must fall on a section of the arc of radius $|\vec{r}_4|$ centered at c that falls between the circles of radius $r_{1\min}$ and $r_{1\max}$ centered at the origin.

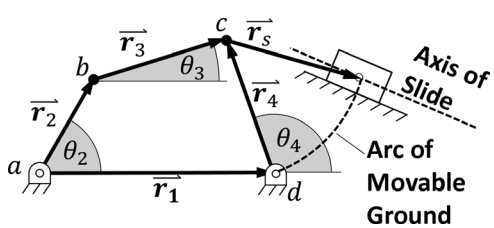

Fig. 1 Variable displacement linkage

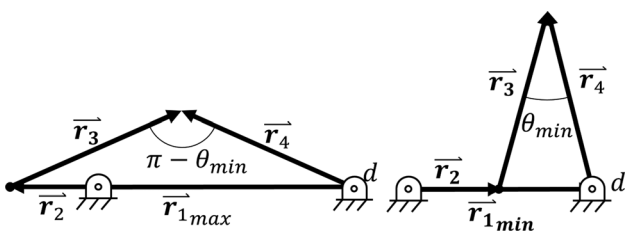

Fig. 2 Base triangles for determining $r_{1\min}$ and $r_{1\max}$

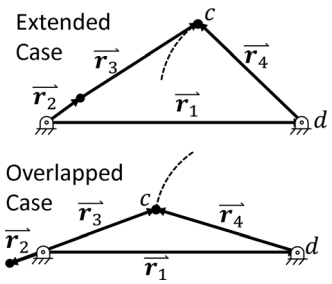

Fig. 3 Extended and overlapped extremes of fourbar linkage

This construction method is satisfied by two arcs, as seen in Fig. 4, both of which are valid as they result in a mirror image of the same linkage. Here, the extended case is shown but the overlapped case is valid as well but will result in the reversal of the TDC and BDC positions of the piston.

2.2.4 Defining Location of Zero Displacement and Axis of Slide. The location of zero displacement can be placed anywhere along the arc of acceptable ground pivots. However, to maximize the displacement range, $|\vec{r}_1|$ should be set to either $r_{1\min}$ or $r_{1\max}$ when determining the location of zero displacement. Doing so means that the position of d associated with zero displacement is located at an extreme of the arc of acceptable ground pivots. This allows maximum travel of d as it moves to the opposite extreme of the arc, creating maximum variability of the linkage.

The axis of slide is coincident with the location of zero displacement as previously described. The angle of the axis of slide is open but the choice affects the maximum slider displacement and transmission angle. The choice of the angle of axis of slide is described in Sec. 2.4.1 by Eq. (7). Because the axis of slide can be defined with the linkage in the extended case or the overlapped case and at $r_{1\max}$ or $r_{1\min}$, there are four configurations in which the linkage can be constructed, which are shown in Fig. 5.

Constructing the slider dyad is done by adding a link equal in length to link 4 called the connecting rod. One end of the connecting rod is pinned to the base fourbar at point c, and the other end is pinned to a slider, which travels along the axis of slide. When d is coincident with the axis of slide, no translation is imparted to the slider because c travels in an arc about the slider. As d moves away from the axis of slide, the path of c varies. As a result, the slider is translated along the axis. The slider will always return to TDC at a specific value of θ_2.

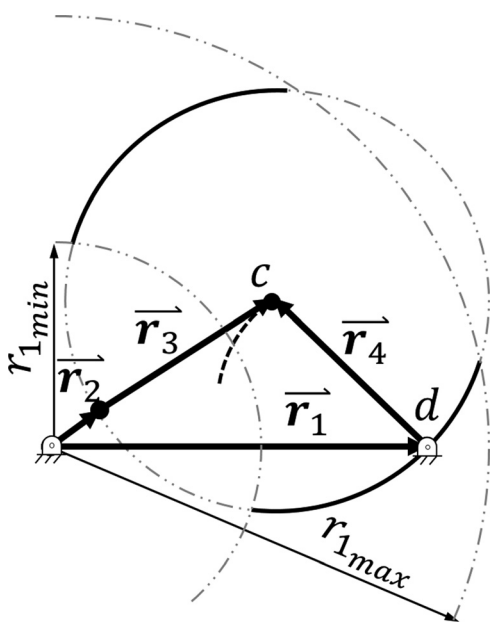

Fig. 4 Variable ground pivot locations for extended case

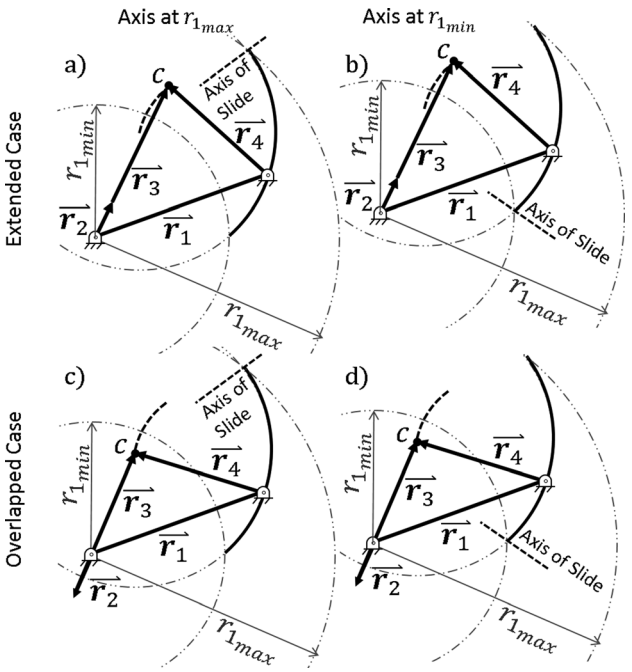

Fig. 5 Configurations of variable linkage

2.3 Kinematic Position Analysis. A position analysis of the adjustable linkage base fourbar will now be presented, which will be used in the performance metrics for evaluating solutions. For the sake of brevity, the following analysis will focus on the geometry shown in Fig. 5(*a*), but the method is universally applicable to the other linkage configurations. For ease of calculation and graphical representation, $\vec{r}_{1\max}$ is set to be collinear with the x-axis and then $\vec{r}_1$ strays off this axis as it travels along the arc of acceptable ground pivots. To find the position of c associated with TDC, a triangle is created, seen in Fig. 6, where $|\vec{r}_{1\max}|$, $|\vec{r}_2|+|\vec{r}_3|$, and $|\vec{r}_4|$ are used to find γ using the law of cosines.

A vector from the origin to point c is defined as

$$\vec{c} = (|\vec{r}_2| + |\vec{r}_3|)e^{i\theta_c} \tag{4}$$

With $\vec{c}$ defined, the arc of acceptable ground pivots can be created. The angle of $\vec{r}_{1\max}$ is defined as 0 deg from the x-axis. The angle of $\vec{r}_{1\min}$ is determined by making another associated triangle, seen in Fig. 6, with sides of $|\vec{r}_{1\max}|$, $|\vec{r}_4|$, and $|\vec{r}_2|+|\vec{r}_3|$.

The law of cosines can then be used to find θ_c. The angle of $\vec{r}_{1\min}$ from the x-axis is then

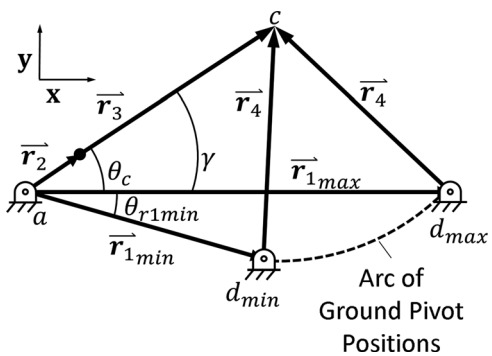

Fig. 6 Associated triangle for determining θ_c and $\theta_{r1\min}$

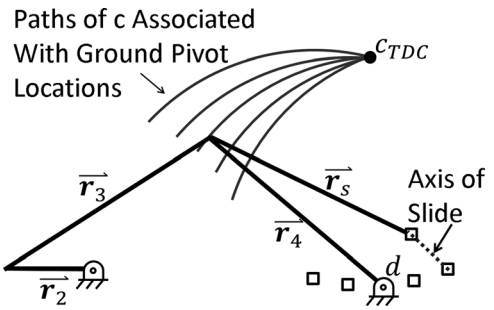

Fig. 7 Variable linkage showing five-ground pivot positions between 0% and 100% displacement and the associated coupler curves

$$\theta_{r1\min} = \gamma - \theta_c \tag{5}$$

Positive θ is read counterclockwise from the x-axis. As drawn in Fig. 6, $\theta_{r1\min}$ has a negative value.

Any point between $\vec{r}_{1\max}$ and $\vec{r}_{1\min}$ at distance of $|\vec{r}_4|$ from point c is an acceptable ground pivot position of the rocker of the fourbar linkage. By repeating this calculation with multiple values of the ground link length and solving the conventional vector loop equations for positional analysis of a fourbar linkage, the resultant adjustable linkage is formed, as seen in Fig. 7 [31].

2.4 Linkage Metrics. A set of performance metrics were developed to evaluate the linkage solutions. These metrics include minimum transmission angle of the base fourbar and slider, maximum displacement of the slider, and footprint area of mechanism. An optimal linkage would have maximum transmission angles, maximum displacement, and minimum mechanism footprint. These performance metrics are now discussed in more detail.

2.4.1 Transmission Angles. A transmission angle is defined as *The acute angle between the relative velocity vectors of the output link and the coupler link* [32]. Force is best transmitted through these links when the transmission angle is 90 deg. There are two transmission angles of interest in this linkage, the angle between links 3 and 4 and the angle between the connecting rod and the slider. The minimum transmission angle between links 3 and 4 was defined earlier in the synthesis by setting the minimum and maximum lengths of the ground link, $|\vec{r}_1|$. The connecting rod to slider transmission angle can be calculated using standard position analysis techniques. The connecting rod to slider transmission angle is dependent on the angle of the axis of slide. With reference to Fig. 8, in the zero-displacement configuration of the linkage, the connecting rod travels in an arc about the slider, defined by the swept angle θ_{4s}. To maximize the slider transmission angle, the angle of the sliding axis should bisect θ_{4s} and is defined as

$$\theta_{\text{As}} = \pi - \theta_{4\max} - \frac{\theta_{4\max} - \theta_{4\min}}{2} \tag{6}$$

where $\theta_{4\max}$ occurs at the overlapped case and $\theta_{4\min}$ occurs at the extended case of the linkage. This selection of the sliding axis is pointed at the center of this arc swung by link 4, as seen in Fig. 8, resulting in an equal transmission at each extreme position at zero displacement. At higher displacements, this is not the case, and as a result, the transmission angle of the slider reaches its minimum value. The angle of slide can be optimized for any displacement by finding the associated θ_{As} at the appropriate position of the movable ground d.

2.4.2 Slider Displacement. The slider displacement is defined as the distance traveled by the slider along the axis of slide from TDC to BDC. The maximum displacement of the slider is calculated when the adjustable ground pivot, d, is located at the furthest

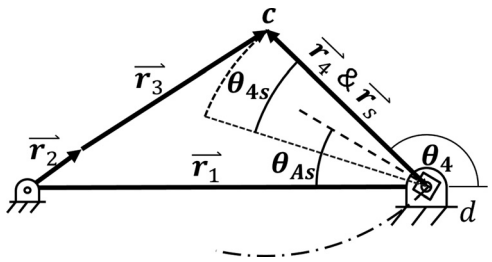

Fig. 8 Defining angle of axis of slide

position from the axis of slide. The maximum displacement can be compared with an inline crank-slider where the displacement of the slider is equal to twice the length of the crank.

2.4.3 Area of Linkage Footprint. The footprint of the linkage is defined as the two-dimensional area occupied by the linkage throughout the range of motion and includes the entirety of the linkage. This area is found by setting the extents of the linkage to a polygon and calculating the internal area. The footprint is guaranteed to be a convex polygon for all cases because the arc of ground pivots extends away from the coupler point c. The units of the footprint are unit length squared.

2.5 Linkage Optimization. The solution space for the linkage involves any of the four configurations previously mentioned, each with any lengths of links 3 and 4. The minimum transmission angle, $\theta_{\min}$, for the revolute joint was set to 30 deg, as suggested by Alt for maintaining good force transmission [33]. Thus, there are two infinities of solutions for each of the four linkage configurations. A grid search optimization study was completed by varying the length of links 3 and 4 through reasonable bounds to determine the linkage metrics described in Sec. 2.4. This study indicated that the minimum slider transmission angle was generally around 60 deg, which is twice that of the recommended minimum. Because of this, the footprint and maximum displacement became the primary optimization metrics of interest. The pump is optimized for energy density by maximizing the ratio of stroke to footprint as follows

$$\max_{r_3, r_4} \frac{\text{stroke}(r_3, r_4)}{\text{footprint}(r_3, r_4)}$$

subject to: $\theta_{\min}(r_3, r_4) > 30\,\text{deg}$

Figure 9 shows a plot of the stroke/footprint for the extended case with the axis of slide located at $r_{1\max}$. The peak of this plot shows the location of the optimum lengths of links 3 and 4 at 2.6 and 2.3 unit lengths, respectively. This study was completed with the other three cases as well. The data for the four optimized

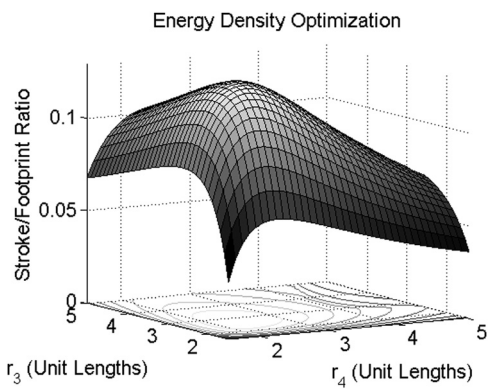

Fig. 9 3D plot of stroke/footprint of case "a" linkage as a function of link lengths R_3 and r_4

Table 1 Linkage optimization results

Configuration	Maximum stroke	Footprint	Stroke/footprint (peak)	Minimum slider transmission angle (deg)
Extended R_{1max}	1.28	9.95	0.13	63
Extended R_{1min}	1.55	8.6	0.18	58
Overlapped R_{1max}	2.1	8.83	0.24	56
Overlapped R_{1min}	1.35	8.74	0.15	52
Crank-slider	2	~5	0.4	~60

linkages and an approximated fixed displacement crank-piston linkage for comparison are presented in Table 1. Based on these data, the overlapped r_{1max} case was selected as it has a superior stroke to footprint ratio and a reasonable minimum slider transmission angle. The optimal length of links 3 and 4 were both found to be 1.8 unit lengths.

2.6 Optimized Linkage Analysis. With the optimized linkage defined, the piston position, velocity, and acceleration of the linkage were analyzed and compared with a fixed-displacement fourbar crank-slider. The velocity is required to calculate the kinetic energy of the mechanism while the acceleration is required to compare the inertial forces. Two vector loop equations are required to solve for the link angles of the sixbar linkage with reference to Fig. 10

$$r_2 e^{i\theta_2} + r_3 e^{i\theta_3} - r_4 e^{i\theta_4} - r_1 e^{i\theta_1} = 0 \tag{7}$$

$$r_4 e^{i\theta_4} + r_5 e^{i\theta_5} - r_6 e^{i\theta_6} - r_7 e^{i\theta_7} = 0 \tag{8}$$

In these two vector equations, the magnitude r_1, r_2, r_3, r_4, r_5, *and* r_6 *are known as well as the angle of the crank link,* θ_2, the *angle of the ground link,* θ_1, and the angle of the axis of slide, θ_7, *which also defines* θ_6. The two equations are solved simultaneously for the four unknowns: θ_3, θ_4, θ_5, and r_7. Therefore, the position of any point on this linkage is resolved.

For comparison purposes, the piston displacement profile of a fixed-displacement inline crank slider is defined as [31]

$$x = r_{crank}\cos(\theta_{crank}) + \sqrt{l_{rod}^2 - r_{crank}^2 \sin^2(\theta_{crank})} \tag{9}$$

The crank radius, r_{crank}, is set equal to the adjustable linkage input link length, r_2, and the length of the connecting rod, l_{rod}, is set equal to the length of link 3 of the optimal sixbar solution.

With the position of the piston known at all crank angles for both the adjustable and fixed linkage, the velocity and acceleration profiles can be calculated from a defined crank angular velocity. The pump is designed to run at a constant angular velocity, ω, of 30π rad/s (1800 rpm). Figures 11 and 12 show the piston velocity and acceleration at 100%, 50%, and 25% of the adjustable linkage along with that of the fourbar crank-slider for comparison. Zero displacement is a flat line along the x-axis because there is no piston motion. These plots show that, while the velocity and acceleration profile of the adjustable linkage differs from that of a fourbar crank-slider mechanism, the values are on the same order of magnitude. In addition, the BDC position of the linkage varies with displacement, and thus the timing ratio varies with displacement as shown in Fig. 13.

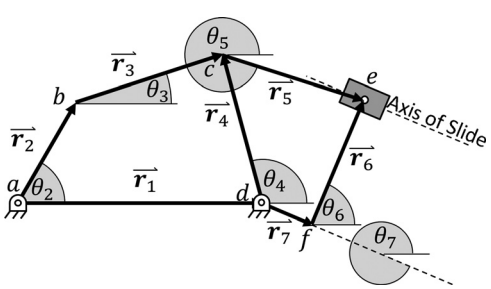

Fig. 10 Sixbar vector loop diagram

3 Experimental Validation

3.1 Experimental System. A prototype linkage was designed and fabricated to be compatible with an existing experimental setup and enable future addition of a pumping cylinder to allow it to function as a variable displacement pump. These design parameters for the pump include a shaft speed of 30π rad/s, maximum flow rate of 15.6 l/min, and a maximum pressure of 6.9 MPa. This flow rate and input speed result in a maximum displacement of 8.67 cm^3/rev. Based on a desire to limit the maximum piston velocity to 3 m/s due to sealing limitations in future experiments, a bore to stroke ratio of 1.32 was chosen. The pin forces were found from the dynamic analysis and piston pressure force. Finally, the link geometry and resulting mass was solved iteratively using the dynamic force analysis.

A prototype machine, shown in Figs. 14 and 15, was built to demonstrate the kinematics and dynamics of the adjustable linkage. The synthesis technique requires that link 4 and the connecting rod to be exactly the same length, which is impossible to realize in actuality. However, if they are not exactly the same but instead within a given tolerance, only a negligible motion of the piston will occur. Figure 16 shows the experimental setup. To measure the piston position, a precision spring with an experimentally determined spring constant was placed between the piston and a force sensor. The measured spring force was used to determine the piston position. The input shaft speed was measured using an optical quadrature encoder.

For the experiment, the angular velocity of the input shaft was limited to 8–10 Hz, which allowed for more points of measurement per revolution. Displacement was varied using a hydraulic

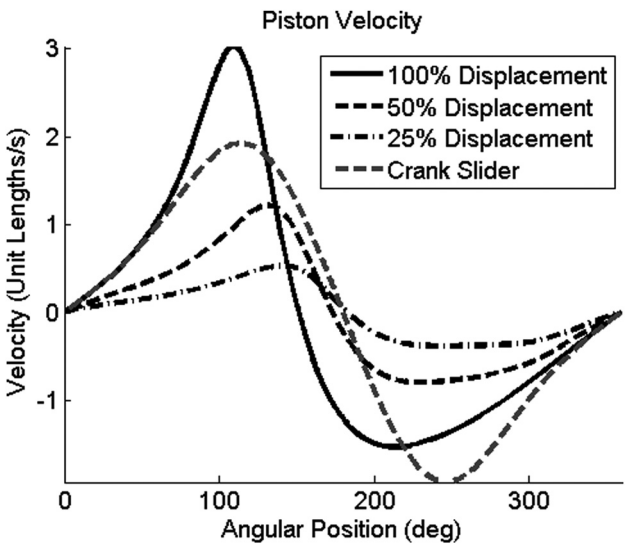

Fig. 11 Piston velocity

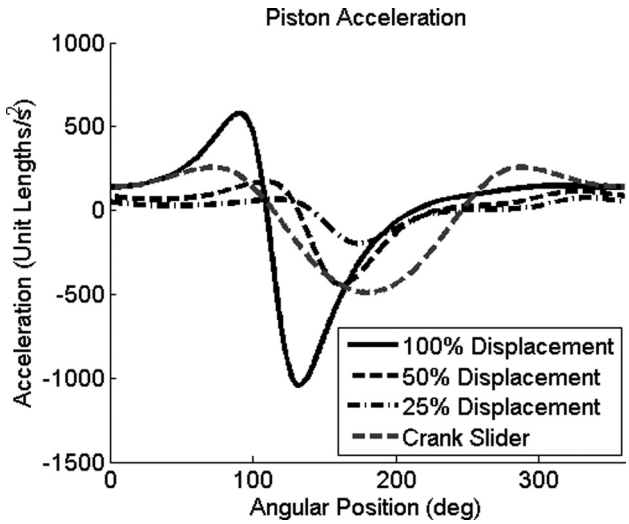

Fig. 12 Piston acceleration

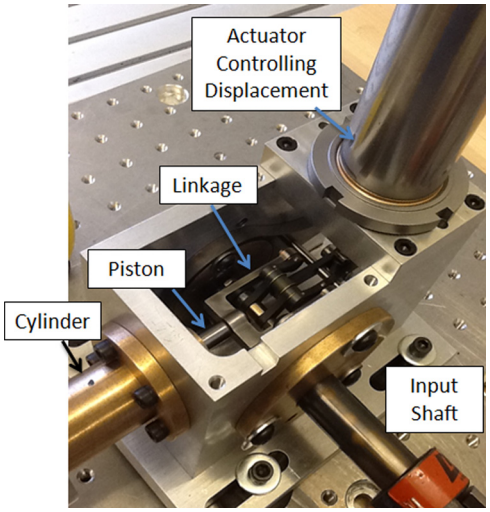

Fig. 15 Prototype variable displacement mechanism

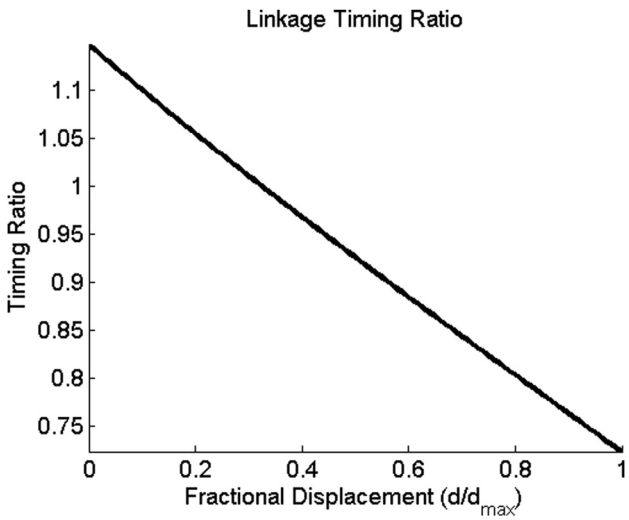

Fig. 13 Linkage timing ratio

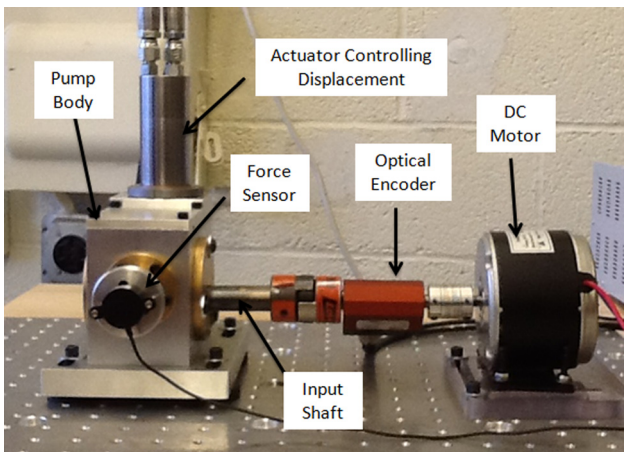

Fig. 16 Experimental setup

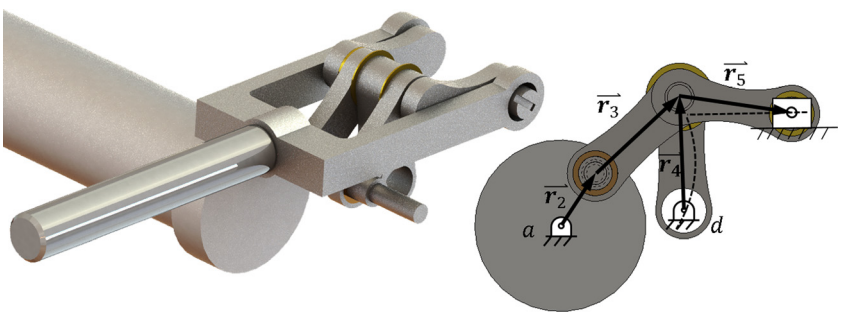

Fig. 14 Prototype linkage cad model and rendering with labeled links

actuator shown in Fig. 16. The percent displacement was determined by dividing the measured piston displacement by the maximum design displacement. Each experiment was run for 5 s and a single crank rotation from TDC position to the next TDC position was selected at random for analysis, but it should be noted that the variation from rotation to rotation was minimal.

3.2 Experimental Results. The angular velocity of the input shaft, seen in Fig. 17, varies between ~340 and 500 rpm through each complete rotation due to the low inertia of the input shaft, the kinetic energy stored in the linkage, and potential energy stored in the spring. The data were filtered digitally using a low pass filter with a cutoff frequency of 50 Hz to remove unwanted 60 Hz noise generated by ac electronics in the room. Since the mechanism was running at 8–10 Hz, this cutoff frequency was deemed acceptable. This filtered crank speed data were then used as an input to the model for an accurate comparison of the position, velocity, and acceleration profiles.

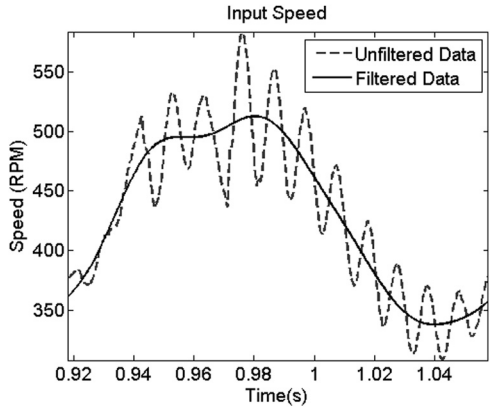

Fig. 17 Input shaft velocity

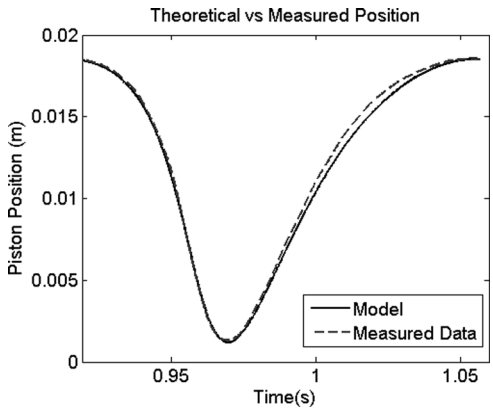

Fig. 18 Piston position

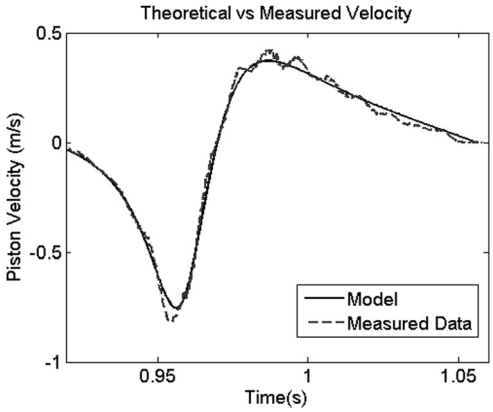

Fig. 19 Piston velocity

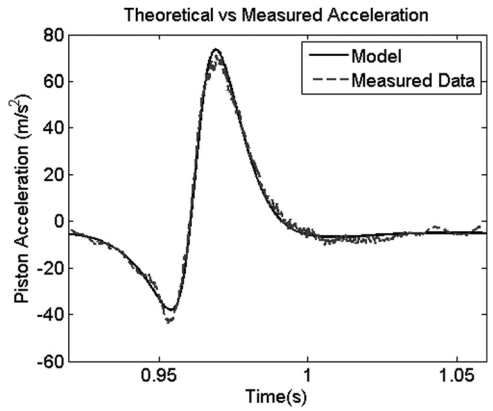

Fig. 20 Piston acceleration

Figure 18 compares the predicted and experimentally measured piston position through one revolution of the input shaft. The BDC position is defined as zero point, and the peak displacement, 0.0185 m, is TDC, which corresponds to 93% of maximum displacement. The x-axis is the time across one revolution of the input shaft. Figures 19 and 20 show the piston velocity and acceleration, respectively, which were created by differentiating the position data. A zero-phase 50-point moving average filter was used to remove the noise created by differentiating experimental data.

4 Discussion

Similarities and differences can be observed in Figs. 11 and 12 between the behavior of the adjustable linkage and that of a fourbar crank-slider mechanisms, which are already used in fixed-displacement reciprocating piston pumps. While the adjustable linkage has a constant TDC position, the BDC position varies with displacement as seen in Fig. 11. As a result, the timing ratio of the linkage varies as seen in Fig. 13.

A timing ratio close to 1 is desirable because it minimizes piston velocities and accelerations. The timing ratio is 1 at 33% displacement and deviates by 15% at zero displacement. At maximum displacement, the timing ratio deviates by 28% from 1. As a result, the maximum acceleration is 2.5 times higher than that of a comparable crank slider with a constant timing ratio of 1. When used in a pumping application, the variable timing ratio is not a problem because check valves can be used to control the fluid flow into and out of the pumping chamber. However, when used in motoring applications, active valves with variable timing are required to synchronize the fluid flow with the varying BDC position. This will be addressed in future work.

The variations in the input shaft velocity, seen in Fig. 17, are due to the kinetic and potential energy storage in the linkage and spring, respectively. When the piston is traveling from TDC to BDC, the spring is extending, which applies torque to the shaft, aiding its rotation, thus increasing its speed. When the piston is returning from BDC to TDC, the spring is compressing and storing energy, requiring additional torque, slowing the dc motor speed. In addition, Fig. 17 shows that the variations in shaft velocity do not correspond exactly to TDC and BDC position. This can be attributed to the kinetic energy change as the links are changing velocity through the cycle.

As shown in Figs. 18–20, the experimental data exhibit excellent agreement with the model predictions. The slight variations observed can be attributed to machining tolerances and measurement accuracy. The choice to display the results from a high displacement was based on a desire to show the largest travel, velocity, and acceleration. Although not shown, experiments run at other displacements exhibited similar results.

5 Conclusions

This paper describes a synthesis technique and experimental validation of an adjustable linkage for use as a variable displacement piston pump/motor that can go to zero displacement and has a constant top dead center. Such a linkage is made by creating a base fourbar with an arc for a coupler curve and attaching a dyad with a slider joint to the end of the follower link. By placing the slider pivot at the ground pivot of the follower, the slider will exhibit zero displacement. When the ground link is moved along an arc about K_{TDC}, the slider will be displaced while returning to a constant TDC. The linkage was optimized for a maximum stroke

and minimum footprint with a minimum base fourbar transmission angle of 30 deg and a minimum slider transmission angle of 52 deg.

The experimental results show that such a linkage can be realized, validated the kinematic model, and gives confidence to the inertial force analysis. The footprint of variable linkages is approximately twice as large as that of a comparable fixed displacement crank-slider, but the increase in size can be expected with the added capability of variable displacement. It is expected that this mechanism will result in a highly efficient pump due to the low friction revolute joints, lack of hydrodynamic bearings, lack of piston side-loading due to the cross-head bearing, and low unswept volume at all displacements. Future work is planned to evaluate the viability of the linkage as a pumping mechanism. This work will help to create and analyze an efficient, variable displacement hydraulic pump, which can be used in many applications.

Acknowledgment

This work is supported by the National Science Foundation Grant No. EFRI-1038294.

References

[1] Williamson, C., Zimmerman, J., and Ivantysynova, M., 2008, "Efficiency Study of an Excavator Hydraulic System Based on Displacement-Controlled Actuators," Proceedings of the Bath/ASME Symposium on Fluid Power and Motion Control.

[2] Li, P. Y., Loth, E., Simon, T. W., Van de Ven, J. D., and Crane, S. E., 2011, "Compressed Air Energy Storage for Offshore Wind Turbines," International Fluid Power Exposition, Las Vegas, NV.

[3] Ivantysyn, J., and Ivantysynova, M., 2001, *Hydrostatic Pumps and Motors*, Academic Books International, New Delhi.

[4] Wieczorek, U., and Ivantysynova, M., 2002, "Computer Aided Optimization of Bearing and Sealing Gaps in Hydrostatic Machines—The Simulation Tool CASPAR," Int. J. Fluid Power, **3**(1), pp. 7–20.

[5] Manring, N. D., 2003, "Valve-Plate Design for an Axial Piston Pump Operating at Low Displacements," ASME J. Mech. Des., **125**(1), pp. 200–205.

[6] Inaguma, Y., and Hibi, A., 2007, "Reduction of Friction Torque in Vane Pump by Smoothing Cam Ring Surface," Proc. Inst. Mech. Eng., Part C: J. Mech. Eng. Sci., **221**(5), pp. 527–534.

[7] Wang, S., 2012, "Improving the Volumetric Efficiency of the Axial Piston Pump," ASME J. Mech. Des., **134**, p. 111001.

[8] Grandall, D. R., 2010, "The Performance and Efficiency of Hydraulic Pumps and Motors," MSc. thesis, The University of Minnesota, Minneapolis, MN.

[9] Seeniraj, G. K., and Ivantysynova, M., "Impact of Valve Plate Design on Noise, Volumetric Efficiency and Control Effort in an Axial Piston Pump," ASME 2006 International Mechanical Engineering Congress and Exposition, Fluid Power Systems and Technology, Chicago, IL, ASME Paper No. IMECE2006-15001, Nov. 5–10, New York, pp. 77–84.

[10] Tao, D. C., and Krishnamoorthy, S., 1978, "Linkage Mechanism Adjustable for Variable Symmetrical Coupler Curves With a Double Point," Mech. Mach. Theory, **13**(6), pp. 585–591.

[11] Tao, D. C., and Krishnamoorthy, S., 1978, "Linkage Mechanism Adjustable for Variable Coupler Curves With Cusps," Mech. Mach. Theory, **13**(6), pp. 577–583.

[12] McGovern, J. F., and Sandor, G. N., 1973, "Kinematic Synthesis of Adjustable Mechanisms (Part 1: Function Generation)," ASME J. Eng. Ind., **95**(2), pp. 417–422.

[13] McGovern, J. F., and Sandor, G. N., 1973, "Kinematic Synthesis of Adjustable Mechanisms (Part 2: Path Generation)," ASME J. Eng. Ind., **95**(2), pp. 423–429.

[14] Handra-Luca, V., 1973, "The Study of Adjustable Oscillating Mechanisms," ASME J. Eng. Ind., **95**(3), pp. 677–680.

[15] Zhou, H., and Ting, K.-L., 2002, "Adjustable Slider-Crank Linkages for Multiple Path Generation," Mech. Mach. Theory, **37**(5), pp. 499–509.

[16] Xu, W., Lewis, D., Bronlund, J., and Morgenstern, M., 2008, "Mechanism, Design and Motion Control of a Linkage Chewing Device for Food Evaluation," Mech. Mach. Theory, **43**(3), pp. 376–389.

[17] Grenier, M., and Gosselin, C., "Kinematic Optimization of a Robotic Joint With Continuously Variable Transmission Ratio," Proceedings of the ASME 2011 International Design Engineering Technical Conferences and Computers and Information in Engineering Conference, Washington, DC, Aug. 28–31, ASME, New York, pp. 513–521.

[18] Patel, S. R., and Patel, D., 2013, "Dynamic Analysis of Quick Return Mechanism Using MATLAB," Int. J. Eng. Sci. Innovative Technol., **2**(3), pp. 346–350.

[19] Shyu, J. H., Chen, C. K., Yu, C. C., and Luo, Y. J., 2011, "Research and Development of an Adjustable Elliptical Exerciser," Adv. Mater. Res., **308**, pp. 2078–2083.

[20] Bai, L., Ge, W.-j., Chen, X.-h., and Meng, X.-y., "Hopping Capabilities of a Bio-Inspired and Mininally Actuated Hopping Robot," 2011 International Conference on Proceedings of the Electronics, Communications and Control (ICECC), Zhejiang, China, Sept. 9–11, IEEE, New York, pp. 1485–1489.

[21] Soong, R.-C., and Chang, S.-B., 2011, "Synthesis of Function-Generation Mechanisms Using Variable Length Driving Links," Mech. Mach. Theory, **46**(11), pp. 1696–1706.

[22] Anirban, G., and Amarnath, C., 2011, "Adjustable Mechanism for Walking Robots With Minimum Number of Actuators," Chin. J. Mech. Eng., **24**(5), p. 760.

[23] Nelson, C. D., 1985, *Variable Stroke Engine*, U.S. Patent 4,517,931.

[24] Pierce, J., 1914, *Variable Stroke Mechanism*, U.S. Patent 1,112,832.

[25] Pouliot, H. N., Delameter, W. R., and Robinson, C. W., 1977, "A Variable Displacment Spark-Ignition Engine," SAE Technical Paper No. 770114, SAE International.

[26] Yamin, J. A. A., and Dado, M. H., 2004, "Performance Simulation of a Four-Stroke Engine With Variable Stroke-Length and Compression Ratio," Appl. Energy, **77**(4), pp. 447–463.

[27] Freudenstein, F., and Maki, E. R., 1981, "Variable Displacement Piston Engine," U.S. Patent 4,270,495.

[28] Freudenstein, F., and Maki, E., 1983 "Development of an Optimum Variable-Stroke Internal-Combustion Engine Mechanism From the Viewpoint of Kinematic Structure," ASME J. Mech., Trans, and Automation, **105**(2), pp. 259–266.

[29] Shoup, T. E., 1984, "The Design of an Adjustable, Three Dimensional Slider Crank Mechanism," Mech. Mach. Theory, **19**(1), pp. 107–111.

[30] Wilhelm, S., and Van de Ven, J. D., 2011, "Synthesis of a Variable Displacement Linkage for a Hydraulic Transformer," Proceedings of the ASME 2011 International Design Engineering Technical Conferences & Computers and Information in Engineering Conference, IDETC/CIE 2011, August 28–31, 2011, Washington, DC, ASME, New York, p. 8.

[31] Norton, R. L., 2008, *Design of Machinery An Introduction to the Synthesis and Analysis of Mechanisms and Machines*, McGraw-Hill, Boston, MA.

[32] Sandor, G. N., and Erdman, A. G., 1984, *Advanced Mechanism Design: Analysis and Sythesis*, Prentice-Hall, Upper Saddle River, NJ.

[33] Alt, V. H., 1932, "The Transmission Angle and Its Importance for the Design of Periodic Mechanisms," Werstattstechnik, **26**, pp. 61–64.